J|A|C|S
ARTICLES
Published on Web 01/12/2007

Temperature-Induced Reversible Morphological Changes of Polystyrene-*block*-Poly(ethylene Oxide) Micelles in Solution

Prachur Bhargava, Yingfeng Tu, Joseph X. Zheng, Huiming Xiong, Roderic P. Quirk, and Stephen Z. D. Cheng*

Contribution from The Maurice Morton Institute and Department of Polymer Science, The University of Akron, Akron, Ohio 44325-3909

Received July 24, 2006; E-mail: scheng@uakron.edu

Abstract: Temperature-induced reversible morphological changes of polystyrene-*block*-poly(ethylene oxide) micelles with degrees of polymerization of 962 for the PS and 227 for the PEO blocks (PS_{962}-*b*-PEO_{227}) in *N*,*N*-dimethylformamide (DMF)/water, in which water is a selective solvent for the PEO block, were observed. For a system with 0.2 wt % copolymer concentration and 4.5 wt % water concentration in DMF/water, the micelle morphology observed in transmission electron microscopy changed from vesicles at room temperature to worm-like cylinders and then to spheres with increasing temperature. Mixed morphologies were also formed in the intermediate temperature regions. Cooling the system back to room temperature regenerated the vesicle morphology, indicating that the morphological changes were reversible. No hysteresis was observed in the morphological changes during heating and cooling. Dynamic light scattering revealed that the hydrodynamic radius of the micelles decreased with increasing temperature. Combined static and dynamic light scattering results supported the change in morphology with temperature. The critical micellization temperatures and critical morphological transition temperatures were determined by turbidity measurements and were found to be dependent on the copolymer and water concentrations in the DMF/water system. The morphological changes were only possible if the water concentration in the DMF/water system was low, or else the mobility of the PS blocks would be severely restricted. The driving force for these morphological changes was understood to be mainly a reduction in the free energy of the corona and a minor reduction in the free energy of the interface. Morphological observations at different time periods of isothermal experiments indicated that in the pathway from one equilibrium morphology to another, large compound micelles formed as an intermediate or metastable stage.

Introduction

Amphiphilic block copolymers can self-assemble to form a variety of micelle morphologies in both aqueous media and organic solvents.[1−9] These colloidal systems have potential applications in pharmaceuticals and separation systems.[10−12] The micelle morphology is tuned by molecular parameters, such as molecular weight and block copolymer composition, and solution parameters like copolymer concentration, solvent composition, temperature, and others.

Temperature has been used as a tool to control the block copolymer self-assembly for several years.[13−20] The nature of the polymer−solvent interactions is important in these studies. If the system displays an upper critical solution temperature (UCST) behavior, micellization takes place below a critical temperature; while if the polymer displays a lower critical solution temperature (LCST) behavior, micellization takes place above a critical temperature. In either case, this temperature is known as the critical micellization temperature (CMT). This temperature-dependent micellization and demicellization is specifically useful for temperature-driven drug delivery.[21]

Because poly(*N*-isopropylacrylamide) (PNIPAM) is known to have an LCST behavior in water, several PNIPAM-based

(1) Nagarajan, R.; Ganesh, K. *J. Chem. Phys.* **1989**, *90*, 5843−5856.
(2) Halperin, A. *Macromolecules* **1987**, *20*, 2943−2946.
(3) Gast, A. P.; Vinson, P. K.; Cogan-Farinas, K. A. *Macromolecules* **1993**, *26*, 1774−1776.
(4) Qin, A.; Tian, M.; Ramireddy, C.; Webber, S. E.; Munk, P.; Tuzar, Z. *Macromolecules* **1994**, *27*, 120−126.
(5) Gao, Z.; Varshney, S. K.; Wong, S.; Eisenberg, A. *Macromolecules* **1994**, *27*, 7923−7927.
(6) Zhang, L.; Eisenberg, A. *J. Am. Chem. Soc.* **1996**, *118*, 3168−3181.
(7) Jain, S.; Bates, F. S. *Science* **2003**, *300*, 460−464.
(8) Zhang, L.; Yu, K.; Eisenberg, A. *Science* **1996**, *272*, 1777−1779.
(9) Geng, Y.; Ahmed, F.; Bhasin, N.; Disher, D. E. *J. Phys. Chem. B* **2005**, *109*, 3772−3779.
(10) Allen, C.; Han, J.; Yu, K.; Maysinger, D.; Eisenberg, A. *J. Controlled Release* **2000**, *63*, 275−286.
(11) Alexandridis, P.; Lindman, B. *Amphiphilic Block Copolymers: Self Assembly and Applications*; Elsevier: New York, 2000; p 305.
(12) Kim, Y.; Dalhaimer, P.; Christian, D. V.; Discher, D. E. *Nanotechnology* **2005**, *16*, 484−491.
(13) Zhou, Z.; Chu, B.; Peiffer, D. G. *Macromolecules* **1993**, *26*, 1876−1883.
(14) Fukumine, Y.; Inomata, K.; Takano, A.; Nose, T. *Polymer* **2000**, *41*, 5367−5374.
(15) Iyama, K.; Nose, T. *Polymer* **1998**, *39*, 651−658.
(16) Solomatin, S. V.; Bronich, T. K.; Eisenberg, A.; Kabanov, V. A.; Kabanov, A. V. *Langmuir* **2004**, *20*, 2066−2068.
(17) Aathimanikandan, S. V.; Savariar, E. N.; Thayumanavan, S. *J. Am. Chem. Soc.* **2005**, *127*, 14922−14929.
(18) Bang, J.; Viswanathan, K.; Lodge, T. P.; Park, M. J.; Char, K. *J. Chem. Phys.* **2004**, *121*, 11489−11500.
(19) Liu, X. M.; Yang, Y. Y.; Leong, K. W. *J. Colloid Interface Sci.* **2003**, *266*, 295−303.
(20) Wei, H.; Zhang, X. Z.; Zhou, Y.; Cheng, S. X.; Zhuo, R. X. *Biomaterials* **2006**, *27*, 2028−2034.

block copolymers have been investigated in this respect.[22−24] The poly(ethylene oxide)-*block*-poly(propylene oxide)-*block*-poly(ethylene oxide) (PEO-*b*-PPO-*b*-PEO) triblock copolymer has also been exhaustively investigated due to its interesting LCST behavior in water.[25−30] At higher concentrations, it also exhibits ordered phases such as cubic, hexagonal, and lamellar phases.[26] Relatively less literature is available on using temperature to control micelle morphologies of block copolymers in dilute solution.[15,31] Pispas and Hadjichristidis investigated the effect of temperature on polybutadiene-*block*-poly(ethylene oxide) (PBD-*b*-PEO) micelle solutions in water by static and dynamic laser light scattering (LLS).[32] They observed a slight increase in the intensity of scattered light and a decrease in the hydrodynamic radius with increasing temperature, but they could not conclude any changes in the micelle morphology. A temperature−concentration phase diagram was mapped for polystyrene-*block*-polydimethlysiloxane (PS-*b*-PDMS), in which PS formed the core and PDMS formed the corona, by Iyama and Nose.[15] Using static and dynamic LLS experiments, they estimated distinct phases of spheres and cylinders with changes in the temperature and polymer concentration. The effect of temperature on micelle morphology has so far mostly been studied by indirect techniques such as small angle neutron scattering, static LLS, and dynamic LLS. Very recently, temperature-induced morphological changes were studied by atomic force microscopy (AFM) for polystyrene-*block*-polyisoprene (PS-*b*-PI) in a selective solvent for the PI blocks.[33] The copolymer composition was specifically chosen to be on the phase boundary of a calculated morphological phase diagram. For two different block copolymer compositions, they observed a rod to sphere change and a vesicle to cylinder change. The changes were shown to be reversible, although they required over 15 h for the forward change to take place and almost a month to change the morphology back completely.

Polystyrene-*block*-poly(ethylene oxide) (PS-*b*-PEO) has been investigated for its micellization behavior for several decades.[34−37] Block copolymers with PEO in the corona are especially attractive due to its biocompatibility.[38] In our recent work, we had shown that the morphology of PS_{962}-*b*-PEO_{227} (the degrees of polymerization of the PS and PEO blocks were 962 and 227, respectively) can be precisely controlled by varying the solvent composition and copolymer concentration.[39] In the present work, we report the reversible morphological changes of PS_{962}-*b*-PEO_{227} induced solely by changing the temperature for fixed copolymer concentration and solvent composition in a DMF/water system. The changes are reversible and require only a few hours of equilibrating for the forward and backward changes. To the best of our knowledge, this is the first direct observation of accessing, solely by changing the temperature, all of the classical micelle phase morphologies in dilute solution (i.e., spheres, cylinders, and vesicles) for a block copolymer with fixed block and solvent composition and at a fixed copolymer concentration. The morphological changes are also monitored for different copolymer and water concentrations in the DMF/water system. An intermediate, or metastable, micelle morphology is also found in the pathway from one thermodynamically stable morphology to another during isothermal experiments. These observations are useful to achieve an insight into the mechanism of these morphological changes.

Results and Discussion

Temperature-Induced Micelle Morphological Changes Observed in TEM. Figure 1 shows the morphological changes induced by increasing temperature for a system with 0.2 wt % PS_{962}-*b*-PEO_{227} copolymer concentration and 4.5 wt % water concentration in DMF/water. At room temperature, the micelle morphology is vesicles as shown in Figure 1a. This is in agreement with the morphological diagram for this system as we have recently reported.[39] At 45 °C, the morphology changes to a mixture of worm-like cylinders and vesicles (Figure 1b). When the temperature is increased to 50 °C, worm-like cylinders are formed exclusively, as shown in Figure 1c. At 60 °C, a mixture of spheres and rod-like cylinders is obtained (Figure 1d), and finally at 70 °C, the morphology changes to aggregated spheres (Figure 1e). The spheres are aggregated because at higher temperatures, the solvent quality of water for PEO is not as good as at room temperature and the PEO chains might be less effective in providing colloidal stabilization to the micelles; therefore, the spheres could be present as an interconnected phase in the solution. On the other hand, the interconnection of the cylinders (Figure 1c) is dependent on the copolymer concentration as presented in our recent work.[40] In that paper, it was shown that at low copolymer concentrations, the cylinders are not connected; while, at high copolymer concentration, they were found to be interconnected, which was supported by TEM and viscosity measurements. Here, it is demonstrated that by changing only the temperature, we can access spherical, worm-like cylindrical and vesicular morphologies without changing compositions of the system. Note that all of these observations of the morphological changes were taken after the samples were equilibrated for 4 h, and thus, they were assumed to be at the equilibrium condition (see the following paragraphs for experimental evidence).

When each of these samples is cooled back to room temperature, the vesicular morphology is regenerated. Detailed morphological studies show that the morphological changes during cooling for the system with 0.2 wt % copolymer

(21) Liu, S. Q.; Tong, Y. W.; Yang, Y. *Biomaterials* **2005**, *26*, 5064−5074.
(22) Liu, X. M; Wang, L.; Huang, J.; He, C. *Biomaterials* **2004**, *25*, 5659−5666.
(23) Andre, X.; Zhang, M.; Mueller, A. H. E. *Macromol. Rapid Commun.* **2005**, *26*, 558−563.
(24) Wei, H.; Zhang, X. Z.; Zhou, Y.; Cheng, S. X.; Zhuo, R. X. *Biomaterials* **2006**, *27*, 2028−2034.
(25) Linse, P. *Macromolecules* **1993**, *26*, 4437−4449.
(26) Glatter, O.; Scherf, G.; Schillén, K. Brown, W. *Macromolecules* **1994**, *27*, 6046−6054.
(27) Michels, B.; Waton, G.; Zana, R. *Colloids Surf., A* **2001**, *183−185*, 55−65.
(28) Su, Y.-L.; Wang, J.; Liu, H.-Z. *Langmuir* **2002**, *18*, 5370−5374.
(29) Waton, G.; Michels, B.; Steyer, A.; Schosseler, F. *Macromolecules* **2004**, *37*, 2313−2321.
(30) Dwyer, C.; Viebke, C.; Meadows, J. *Colloids Surf., A* **2005**, *254*, 23−30.
(31) Chen, E.; Xia, Y.; Graham, M. J.; Foster, M. D.; Mi, Y.; Wu, W.; Cheng, S. Z. D. *Chem. Mater.* **2003**, *15*, 2129−2135.
(32) Pispas, S.; Hadjichristidis, N. *Langmuir* **2003**, *19*, 48−54.
(33) LaRue, I.; Adam, M.; Pitsikalis, M.; Hadjichristidis, N.; Rubinstein, M.; Sheiko, S. S. *Macromolecules* **2006**, *39*, 309−314.
(34) Franta, E. *J. Chim. Phys.* **1966**, *63*, 595−602.
(35) Riess, G.; Rogez, D. *Polym. Prepr.* **1982**, *23*, 19−20.
(36) Yu, K.; Eisenberg, A. *Macromolecules* **1996**, *29*, 6359−6361.
(37) Bronstein, L. M.; Chernyshov, D. M.; Timofeeva, G. I.; Dubrovina, L. V.; Valetsky, P. M.; Obolonkova, E. S.; Khokhlov, A. R. *Langmuir* **2000**, *16*, 3626−3632.
(38) Dunn, S. E.; Brindley, A.; Davis, S. S.; Davies, M. C.; Illum, L. *Pharm. Res.* **1994**, *11*, 1016−1022.
(39) Bhargava, P; Zheng, J. X.; Li, P.; Quirk, R. P.; Harris, F. W.; Cheng, S. Z. D. *Macromolecules* **2006**, *39*, 4880−4888.
(40) Bhargava, P; Zheng, J. X.; Li, Quirk, R. P.; Cheng, S. Z. D. *J. Polym. Sci., Part B:Polym. Phys.* **2006**, *44*, 3605−3611.

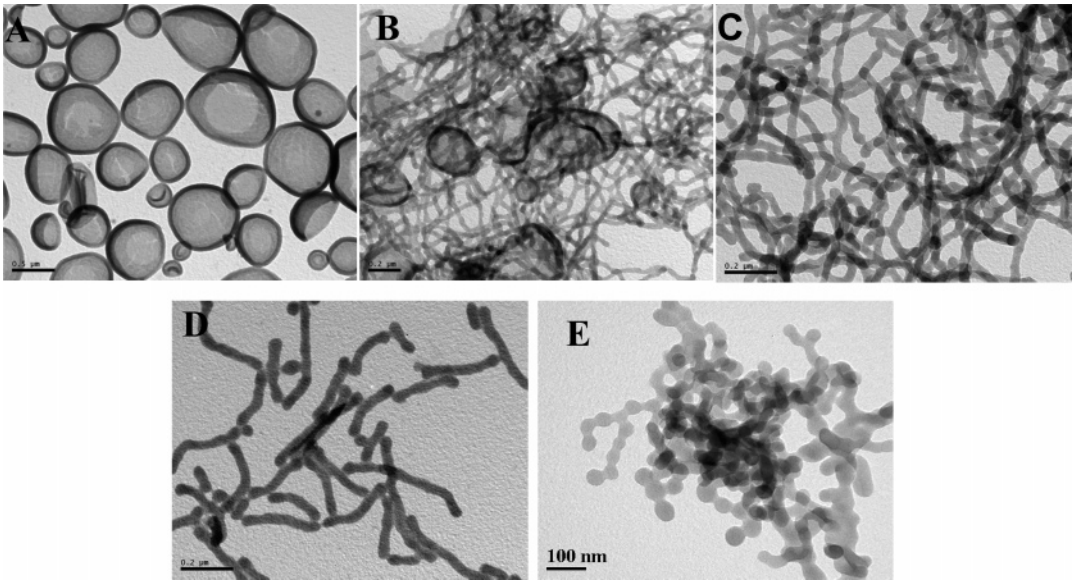

Figure 1. Morphological changes on heating of a system with 0.2 wt % copolymer and 4.5 wt % water concentration in DMF/water: (a) pure vesicles formed at room temperature; (b) a mixture of vesicles and worm-like cylinders at 45 °C; (c) pure worm-like cylinders at 50 °C; (d) a mixture of spheres and rod-like cylinders at 60 °C; and (e) pure spheres at 70 °C.

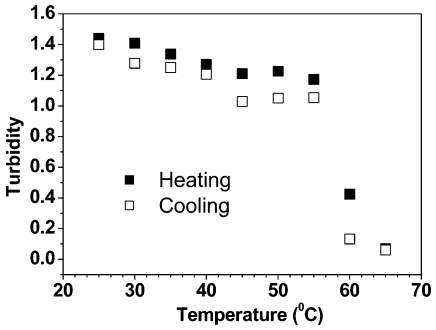

Figure 2. Change in turbidity with temperature for a micelle system with 0.4 wt % copolymer concentration and 4.35 wt % water concentration in DMF/water during heating and cooling.

concentration and 4.5 wt % water concentration in DMF/water are completely reversible. Namely, the TEM morphological observations are from Figure 1e back to Figure 1a during cooling. Furthermore, no hysteresis has been observed during cooling as compared with those observations during heating. This indicates that the time required to conduct the morphological changes during heating and cooling are close to identical.

We also follow the change in turbidity when a system with 0.4 wt % copolymer concentration and 4.35 wt % water concentration in DMF/water is heated from room temperature and cooled from high temperatures as shown in Figure 2. It is evident that the turbidity changes during heating and cooling are identical, again, indicating the absence of hysteresis in the morphological changes.

Micelle rings are sometimes formed and observed when the vesicles change toward the cylinders. Figure 3a shows the rings coexisting with the vesicles. These were obtained after heating the system with 0.2 wt % copolymer concentration and 4.5 wt % water concentration in DMF/water from room temperature to 40 °C. Initially, the cylinders formed would be short and rod-like, and thus, the end-capping energy would be important as compared to the overall free energy of the micelle. To decrease the overall free energy by eliminating the ends, the rings form if the bending energy is less significant as compared to the end-capping energy. We have also captured some intermediate morphologies for the vesicle to cylinder change. Figure 3b,c shows lamellae with protruding rods, suggesting that rods are formed from the lamellae that originate from the vesicles. Lamellae with protruding rods have also been observed previously for PS-*b*-PEO.[36] We also observed vesicles with protruding rods (Figure 3d), which provides some evidence that the rods may also be occasionally formed directly from the vesicles, although this morphology is only seen rarely.

Micelle Object Size Changes Deduced from LLS. For dynamic LLS experiments, the cumulant analysis of the measured intensity−intensity time-correlation function of the distributed object can lead to an accurate average line width $<\Gamma>$.[41,42] For a purely diffusive relaxation, Γ is related to the translational diffusion coefficient D by

$$D = (\Gamma/q^2)_{q\to 0} \tag{1a}$$

or the hydrodynamic radius, R_h, by

$$R_h = k_B T/(6\pi\eta D) \tag{1b}$$

where q is the scattering wave vector, k_B is the Boltzmann constant, η is the solution viscosity, and T is the absolute temperature. The hydrodynamic diameter, D_h, can be deduced by $D_h = 2R_h$. In static LLS experiments, the excess time-averaged scattering light intensity, $I_{ex} = I_s$(solution) − I_s-(solvent), can be used to deduce the excess Rayleigh ratio, R_{ex}, from

$$R_{ex} = I_{ex}R^2/I_{INC} \tag{2}$$

where R and I_{INC} are the Rayleigh ratio and incident laser intensity, respectively. In the dilute solution regime, the classical

(41) Chu, B. *Laser Light Scattering: Basic Principles and Practice*, 2nd ed.; Academic Press: San Diego, 1991.
(42) Brown, W. *Light Scattering: Principles and Development*; Oxford University Press: New York, 1996.

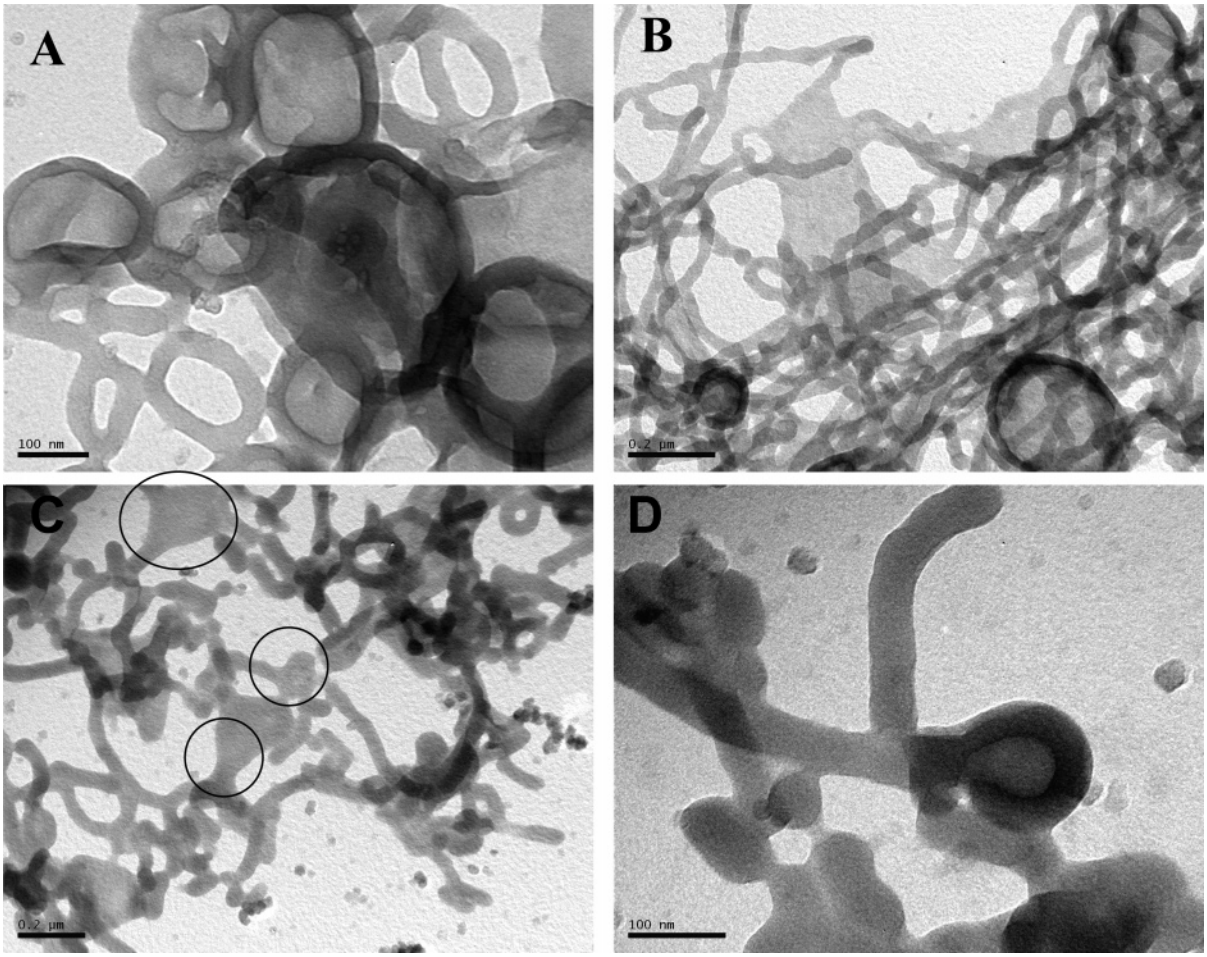

Figure 3. Intermediate morphologies formed on heating a system with 0.2 wt % copolymer and 4.5 wt % water concentration in DMF/water: (a) a mixture of vesicles and rings at 40 °C; (b) lamellae with protruding rods at 45 °C; (c) circular lamellae with protruding rods; and (d) vesicles with protruding rod.

Zimm equation holds

$$\frac{KC}{R_{ex}} \cong \frac{1}{MP(q)} + 2A_2C \tag{3a}$$

where K, C, M, $P(q)$, and A_2 are the optical constant, the polymer concentration, the particle molar mass, the particle scattering factor (also know as the form factor), and the second virial coefficient, respectively. For mono-disperse small particles ($qR_g \ll 1$)

$$P(q) = 1 - q^2R_g^2/3 \tag{3b}$$

where R_g is the radius of gyration of the scattering objects.

The micelle object size changes for a 0.2 wt % copolymer concentration and 4.5 wt % water content DMF/water mixture were also monitored by static and dynamic LLS experiments at different temperatures. Figure 4 shows the change in hydrodynamic radius with temperature obtained by dynamic LLS and analyzed by CONTIN (a program using the constrained regulation method). At 20 °C, the micelle objects are very large with an average diameter of 660 nm. Compared to the TEM images, this size value corresponds to the average diameter of the vesicles. When the temperature increases to 40 °C, the average object size decreases to 470 nm. At 60 °C, the size decreases to 90 nm. With only these results, it is difficult to predict that this decrease in the hydrodynamic radius of the objects is caused by the shrinking of the vesicles or the change of vesicles to other morphologies. Combined with the TEM observations, it is evident that the size change is associated with the morphological change from vesicles to worm-like cylinders.

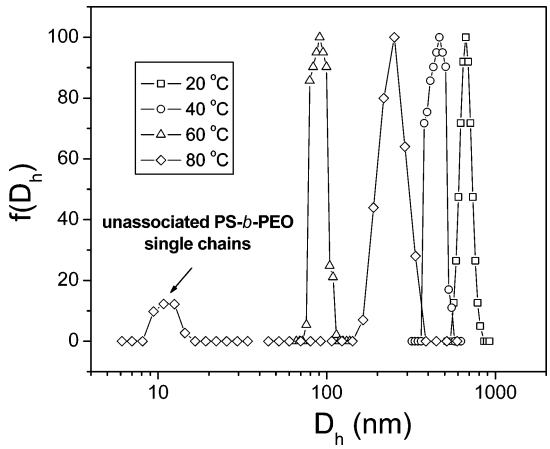

Figure 4. Temperature dependence of the hydrodynamic diameter distribution, $f(R_h)$, for the micelles in the DMF/water mixture.

The static LLS experimental results also provide support of the morphology changes. In the system we studied, the object size is very large, and we were unable to measure a range of

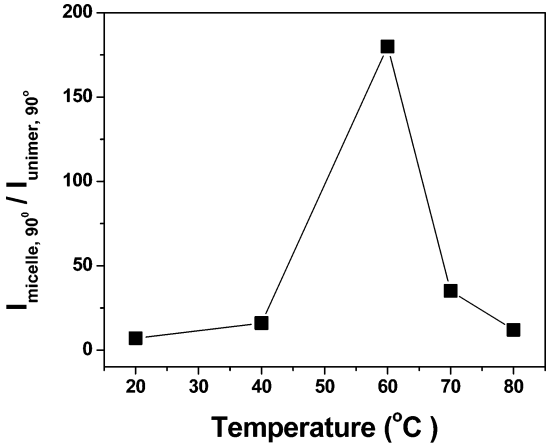

Figure 5. Temperature dependence of the ratio of scattering intensities ($I_{micelle,90°C}/I_{unimer,90°C}$) measured at 90 °C, where $I_{micelle,90°C}$ is for the copolymer in the DMF/water mixture and $I_{unimer,90°C}$ is in the pure DMF solution, $I_{unimer,90°C}$.

scattering angles where $qR_g \ll 1$ (at all angles we measured are in the $qR_g > 1$ range). Since the molar mass and the scattering factor of the particles in this micellar system are very large, the term A_2C in eq 3a can be neglected. This results in the following simplification:

$$\frac{KC}{R_{ex}} \cong \frac{1}{MP(q)} \tag{4}$$

If the scattering angle is fixed at 90° (thus, q is constant) and the concentration of the polymer along with other physical constants does not change significantly after water is added (i.e., only the particle size and particle molar mass changes significantly), we can compare the micelle solution to the pure polymer unimer solution in DMF. Substituting eq 4 into eq 2, we can obtain

$$\frac{I_{ex,micelle}}{I_{ex,unimer}} = \frac{R_{ex,micelle}}{R_{ex,unimer}} = \frac{M_{micelle}P(q)_{micelle}}{M_{unimer}P(q)_{unimer}} \tag{5}$$

Therefore, from the change of the scattering intensity at 90°, we can observe the trend of the change in particle molar mass and the form factor. In Figure 5, we plot the ratio of scattering intensity of the copolymer in the DMF/water mixture ($I_{micelle,90°C}$) to the scattering intensity of copolymer in pure DMF ($I_{unimer,90°C}$) at different temperatures.

In Figure 5, as the temperature rises from 20 to 40 then to 60 °C, the relative intensity ratio increases. This implies that either the molar mass of the micelle increases, that the scattering vector increases, or both. This is contrary to the dynamic LLS results that indicate that the object size decreased during heating. The only possible explanation is that the object morphology changes when the temperature increases. If the object morphology does not change, the object molar mass cannot increase with decreasing the object size. Coupled with the TEM observations, we are able to conclude that there is a morphological change of vesicles to cylinders with increasing temperature. The cylinders have a larger molar mass than the vesicles but a smaller hydrodynamic diameter. This is similar to a smaller-sized rod being heavier than a bigger-sized balloon. In our case, it is indeed a very interesting phenomenon.

When the temperature is increased above 60° (such as at 80 °C in Figure 4), some of the block copolymer can be dissolved in the mixed solvent, as seen as the small bump around 10 nm in Figure 4. This leads to the decrease of the scattering intensity in this figure. The larger hydrodynamic diameter particles at 80 °C may be caused by the pearl-necklace-like spheres observed in the TEM images (Figure 1e).

Driving Force for the Morphological Changes. The morphological changes are based on the free energy of the micelle, which consists of the free energy of the core, free energy of the corona, and free energy of the interface.[43] To better understand these changes, we should obtain insight into the PS and PEO interactions with the solvents and how they are affected by changing the temperature. The polymer−solvent interactions can be estimated by the polymer−solvent interaction parameters if we neglect the entropic contribution. These parameters can be estimated using the van Laar−Hildebrand equation[44]

$$\chi_{P-S} = V_S/(RT)(\delta_P - \delta_S)^2 \tag{6}$$

where V_S is the molar volume of solvent and δ_P and δ_S are the solubility parameters of polymer and solvent, respectively. For the sake of simplicity, we neglect the temperature dependence of δ_P, δ_S (they are slightly temperature dependent[44]), and V_S in our calculations. By definition, eq 6 predicts a decrease in the χ_{P-S} value as the temperature increases. By substituting the values in, it is seen that the relative decrease in $\chi_{PS-water}$ is much more significant than the χ_{PS-DMF} and $\chi_{PEO-DMF}$. It is known that PEO has an LCST behavior in water with an LCST temperature around 100 °C and that $\chi_{PEO-water}$ increases as the temperature increases.[45] Therefore, for a 4.5 wt % water concentration in the DMF/water system with an assumption that the system obeys the ideal solution behavior (the solubility parameters in the mixture obey a linear addition scheme), the change in $\chi_{PS-solvent}$ and $\chi_{PEO-solvent}$ with temperature can be calculated. Our calculations reveal that at room temperature, the value of $\chi_{PS-solvent}$ is much higher than $\chi_{PEO-solvent}$, indicating that the solvent mixture (DMF/water) is poor for PS blocks and good for PEO blocks. As the temperature increases, $\chi_{PS-solvent}$ decreases, and the mixed solvent becomes less poor for PS blocks. On the other hand, $\chi_{PEO-solvent}$ does not change significantly with temperature since $\chi_{PEO-water}$ increases and $\chi_{PEO-DMF}$ decreases with increasing temperature. Thus, the overall solvent mixture $\chi_{PEO-solvent}$ remains almost constant.

We can also further examine the solvent quality for PEO by analyzing the change in the excluded volume parameter, v, with temperature. The excluded volume parameter is related to the second virial coefficient, A_2, by the following expression:[46]

$$v = 2A_2M_0/a^3N_{av} \tag{7}$$

where M_0 is the molecular weight of the PEO monomer and N_{av} is Avogadro's number. The second virial coefficient is

(43) Zhang, L.; Eisenberg, A. *Polym. Adv. Technol.* **1998**, *9*, 677−99.
(44) Barton, A. F. M. *Handbook of Polymer−Liquid Interaction Parameters and Solubility Parameters*; CRC Press: Boca Raton, FL, 1990; p 12.
(45) Venohr, H.; Fraaije, V.; Strunk, H.; Borchard, W. *Eur. Polym. J.* **1998**, *34*, 723−732.
(46) Rubinstein, M.; Colby, R. H. *Polymer Physics*; Oxford University Press: Oxford, 2003.

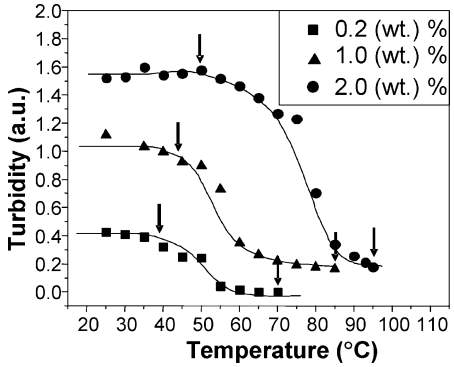

Figure 6. Change in turbidity with temperature for micelle systems with 4.5 wt % water concentration and different copolymer concentrations in DMF/water systems.

related to χ_{P-S} by[47]

$$A_2 = V_{01}(1/2 - \chi_{P-S})/M_0^2 - (V_{01} - V_{02})/(M_n M_0) \quad (8)$$

where V_{01} is the molar volume of the solvent, χ_{P-S} is the interaction parameter, V_{02} is the molar volume of the PEO monomer, and M_n is the number average molecular weight of the PEO polymer. We have already estimated $\chi_{PEO-solvent}$, and using eqs 7 and 8, we can calculate the excluded volume parameter at different temperatures, assuming that all other values are independent of temperature. After calculating and plotting the data, we find that the change in v with temperature is insignificant; therefore, the interaction between PEO and mixed solvent is kept almost unchanged with changing temperature.

The micelle free energy of the system at different temperatures can be calculated based on the size and geometry information obtained from the TEM observations and equations we have described in our recent publication.[39] It is surprising that even though there is a reduction in $\chi_{PS-solvent}$ and a corresponding reduction in the surface tension (γ), the calculated free energy of the interface ($F_{interface}$) remains almost constant for micelles formed at different temperatures. This is because the interfacial area per chain, s, increases from vesicles to cylinders and then to spheres. Therefore, as the temperature is increased, γ decreases, but the area each chain occupies, s, increases. Thus, $F_{interface} = \gamma s$ possesses little change. It can be concluded that the free energy of the interface should not be the major driving force for the micelle morphological changes.

We have found that there is a decrease in the free energy of the corona (F_{corona}), which is dependent mainly on the excluded volume parameter and the tethering density ($1/s$).[39] Previous calculations conducted here, using eqs 7 and 8, revealed that the excluded volume parameter does not change significantly with temperature but that the tethering density ($1/s$) decreases from vesicles to cylinders to spheres. Therefore, it is speculated that the change of F_{corona} acts as the major driving force for the morphological changes with temperature as compared to the case of changing the selective solvent concentrations where the change in $F_{interface}$ is the major driving force for the morphological changes.[39]

Table 1. Morphologies Formed at Different Temperatures for Different Copolymer Concentrations and 4.5 wt % Water Concentration

polymer concentration wt %	temp (°C) 25	40	50	60	70	80
0.2	V[a]	V + C	C	C + S	S	
0.4	V	V	V + C	C	C + S	C + S
2	V	V	V + C	V + C	C	C + S

[a] V: vesicles; C: cylinders; and S: spheres

Initial Copolymer Concentration Effects on the Morphological Changes. We have also followed the morphological changes with temperature for different initial copolymer concentrations while keeping the water concentration fixed at 4.5 wt %. Figure 6 shows the turbidity measurements for 0.2, 1, and 2 wt % copolymer micelle systems with changes in temperature. We can define two characteristic temperatures from these three sets of data. The first temperature is the critical transition temperature (CTT), which is the minimum temperature above which the morphological changes can occur. The second is the critical micellization temperature (CMT), which is the temperature above which no micelles exist. From these three sets of data, both CTT and CMT are dependent on the copolymer concentration. As the copolymer concentration is increased, both CTT and CMT shift to higher temperatures. The CTT values for 0.2, 1, and 2 wt % are 40, 45, and 50 °C, while the CMT values are above 70, 85, and 95 °C, respectively (the vertical arrows in Figure 6).

The results of the micelle morphological changes in the systems having a DMF/water mixture with 4.5 wt % water concentration and different copolymer concentrations are summarized in Table 1. It is evident that the individual morphological changes are shifted to higher temperatures as the copolymer concentration is increased. For example, for 0.2, 0.4, and 2 wt % copolymer concentrations, the rod-like cylindrical morphology is formed at 50, 60, and 70 °C, respectively. Above 80 °C, for the 0.2 wt % copolymer concentration, no micelles exist; while, for 0.4 and 2 wt %, the micelle morphology is still a mixed morphology of spheres and rod-like cylinders. The effect of concentration can be understood on the basis of aggregation number and the polymer−solvent interaction parameter, χ_{P-S}. The aggregation number N_{agg} is related to the concentration from the surfactant theory in small molecules[43]

$$N_{agg} = 2(C/CMC)^{1/2} \quad (9)$$

where C is the surfactant concentration (here, we use the copolymer concentration) and CMC is the critical micellization concentration. This equation is valid for simple micelle morphologies of spheres, rods, and vesicles, although N_{agg} is less sensitive to C in the case of spheres.[48] In our case, the CMC is actually a function of the water concentration, which is an inverse relationship.[39] Therefore, as the copolymer concentration increases, N_{agg} increases. At higher aggregation numbers, the micelle size becomes large, resulting in higher core chain stretching, and thus, a greater reduction in the free energy of the interface is required to stabilize the micelle morphology.

(47) Adames, W.; Breuer, W.; Michalczyk, A.; Borchnard, W. *Eur. Polym. J.* **1989**, *25*, 947−950.

(48) Israelachvili, J. N. *Intermolecular and Surface Forces*, 2nd ed.; Academic Press: London, 1992; pp 241−258.

This can now be achieved by increasing the temperature. Moreover, it is known that the polymer−solvent interaction parameter χ_{P-S} is related to the polymer concentration ϕ by the following equation:[44]

$$\chi_{PS} = \chi_0 + \chi_1\phi + \chi_2\phi^2 + ... \quad (10)$$

where χ_0, χ_1, χ_2... are empirical coefficients. At low copolymer concentrations, the higher order terms are negligible, but at high concentrations, they become important and increase the effective χ_{P-S}. Thus, when the copolymer concentration increases, χ_{P-S} increases. At this condition, the micelle systems need to be heated to higher temperatures to cause a sufficient decrease in χ_{P-S}, which will lead to the morphological changes.

Effect of Water Concentration on the Morphological Changes. We have investigated the morphological changes using TEM for a 0.1 wt % copolymer concentration with different water concentrations, 6, 8, and 10 wt % in DMF/water mixtures. We found that the morphology changes from vesicles to worm-like cylinders and then to a mixture of spheres and rod-like cylinders, when the water concentrations are 6 and 8 wt %. However, the vesicular micelle morphology does not change in the system with the water concentration of 10 wt % even up to 90 °C. We can use eq 6 to predict the change in $\chi_{PS-solvent}$ with temperature for different water concentrations in DMF/water mixtures (see Figure S1 in the Supporting Information). The $\chi_{PS-solvent}$ decreases significantly for all these three water concentrations on increasing the temperature. Therefore, the reduction in the free energy of the interface must be similar in all three systems. The reason for the fact that no morphological changes are seen in the case of 10 wt % water cannot be attributed to the thermodynamic considerations.

In another aspect, we can consider that the mobility of PS blocks could be severely restricted due to its strong hydrophobic nature even though the temperature is close to its T_g. Mobility of PS blocks (which is enhanced by a good solvent DMF) is a necessary condition for the observation of the morphological changes. At higher water concentrations, mobility of PS chains would be restricted, and thus, the morphological changes cannot take place.

Pathways of Morphological Changes in Temperature-Jumping Experiments. To investigate whether the morphological change pathways are identical from different initial micelle phases, we monitored the morphological changes at an isothermal temperature after both rapid heating from room temperature or rapid cooling from a high temperature. A system with 0.4 wt % PS_{962}-*b*-PEO_{227} copolymer concentration and 4.35 wt % water concentration in DMF/water was used. The initial morphology was vesicles at room temperature. First, this system was rapidly heated from room temperature to 50 °C and equilibrated there for 2 h. The morphology observed was mainly worm-like cylinders (TEM image in Figure S2a of the Supporting Information). The second experiment was that the same system was first heated to 80 °C and equilibrated for 2 h, where spherical micelles formed. This system was then quenched to 50 °C and equilibrated for another 2 h. The morphology observed was also mainly worm-like cylinders (TEM image in Figure S2b in the Supporting Information). Different from the first experiment, the cylinders were formed from the spherical micelles, and the system was quenched from a high temperature of 80 °C. Therefore, irrespective of the initial morphology (vesicles or spheres) and the initial temperature (room temperature or 80 °C) of the system from which the morphology at 50 °C was accessed, the identical worm-like cylinder morphology was formed. The morphology at a particular temperature is independent of the initial phases and thermal histories of the systems. Therefore, the micelle morphologies obtained are thermodynamically stable.

We still have a question in our mind: what are the pathways of these two morphological changes when the micelle system is brought from room temperature or from a higher temperature to 50 °C? We first tried to determine the minimum time required at 50 °C to achieve the thermodynamically stable micelles. Within this minimum time, we had the opportunity to catch the intermediate, or metastable, morphologies during the morphological change to the worm-like cylinders. Namely, we wanted to observe the morphological changes with time after the system was quickly brought to 50 °C.

Again, a system with 0.4 wt % copolymer concentration and 4.35 wt % water concentration in DMF/water at room temperature was quickly heated to 50 °C. The morphological changes were observed in TEM after time periods of 30 min, 50 min, 1 h, and 2 h, and the respective morphologies are shown in Figure 7a−d. At 30 min (Figure 7a), we surprisingly observed large compound micelles, which were not found in any of our previous equilibrium micelle morphologies. At a time of 50 min, the morphology became mostly worm-like cylinders mixed with some large compound micelles (Figure 7b). After 1 h, the morphology observed was exclusively worm-like cylinders (Figure 7c), and this morphology did not change with a longer period of time such as 2 h as shown in Figure 7d. Therefore, a period of 1 h is the minimum time required to obtain the thermodynamically stable morphology.

In the next experiment, the system was first rapidly heated to 65 °C to obtain mixed micelles of spheres and rod-like cylinders and equilibrated for 2 h. It was then quenched to 50 °C. We began to monitor the morphology formed after 30 min, 1 h, and 2 h. (The TEM images are shown in Figures S3a−c in the Supporting Information). At a period of 30 min, we also observed large compound micelles that were similar to those we observed in Figure 6a where the system was heated from room temperature. After 1 h, the rod-like cylindrical morphology was formed and retained the same morphology after 2 h. Therefore, the time required to equilibrate the micelle morphology for the system cooled from a higher temperature is identical to that required for the system heated from room temperature. We can conclude that there is no hysteresis in the morphological changes in these isothermal experiments, regardless of whether the system is brought to 50 °C from rapid heating or cooling.

Large compound micelles have been previously observed in several block copolymers including PS_{240}-b-PEO_{180},[36] polystyrene-*block*-poly(acrylic acid), PS_{200}-*b*-PAA_4, in which the hydrophilic block is very small,[6] and polystyrene-*block*-poly(4-vinylpyridine), PS_{306}-*b*-$P4VP_{126}$.[49] Eisenberg et al. have shown that these large compound micelles are reverse micelles in an almost continuous PS phase in the bulk and hydrophilic chains on their surface, which provide colloidal stabilization.[6]

We observe that the large compound micelles are formed during the isothermal experiments after heating a vesicle

(49) Liu, L.; Yong, G.; Cong, Y.; Li, B.; Han, Y. *Marcomol. Rapid Commun.* **2006**, *27*, 260−265.

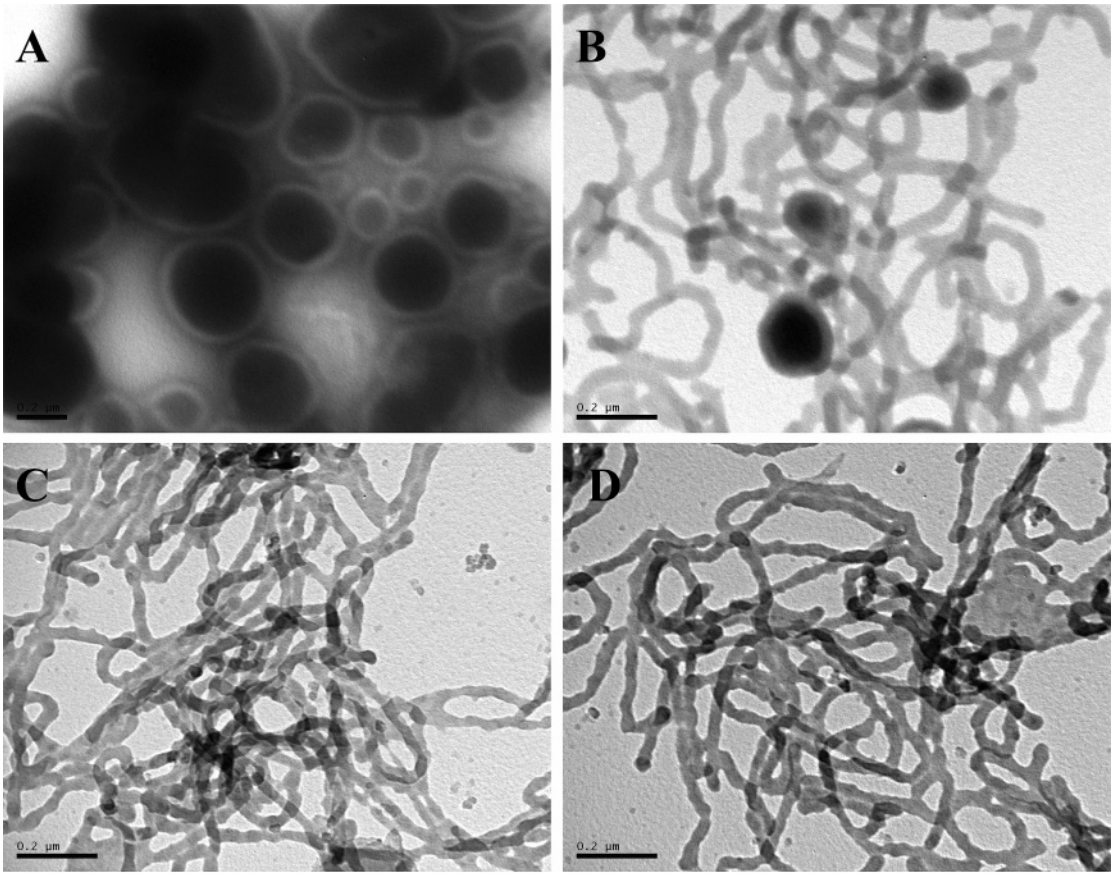

Figure 7. After heating a system with 0.4 wt % copolymer concentration and 4.35 wt % water concentration in DMF/water in which the original morphology was vesicles to 50 °C, the morphological changes with time are (a) large compound micelles after 30 min; (b) mixed large compound micelles and rod-like cylindrical micelles after 50 min; (c) rod-like cylindrical micelles after 1 h; and (d) rod-like cylindrical micelles after 2 h.

morphology system from room temperature to 50 °C or cooling a system with the mixed sphere and worm-like cylinder morphology from 65 to 50 °C. These large compound micelles are not thermodynamically stable and gradually change to rod-like cylindrical micelles.

We wanted to determine whether the large compound micelles can also appear when the system is heated to even higher temperatures. We rapidly heated a vesicle system to 70 °C and monitored the morphological change of micelles with time. The morphology changed from original vesicles to cylinders and spheres (TEM image in Figure S4a in the Supporting Information) after 15 min. After 30 min, as shown, these long cylinders became rod-like short cylinders and spheres (TEM image in Figure S4b in the Supporting Information). No large compound micelles at 70 °C were observed. Therefore, the large compound micelle morphology for PS_{962}-*b*-PEO_{227} is, at best, a thermodynamically metastable morphology.[50,51] This also indicated that the pathways of the morphological changes may be temperature dependent. Further research will be conducted for understanding the pathways of these morphological changes at different temperatures and times.

Conclusion

In summary, we have observed via TEM experiments reversible morphological changes of PS_{962}-*b*-PEO_{227} in DMF/water systems solely by changing the temperature. On increasing the temperature from room temperature, the morphology changed from vesicles to worm-like cylinders and then to spheres with mixed morphologies in between. During cooling of the system from high temperatures, the micelle morphologies returned from spheres to worm-like cylinders and finally reached vesicles at room temperature. No hysteresis was found in the morphological changes achieved by heating and cooling the system. The change in morphology with temperature was supported by static and dynamic LLS experimental results. The critical transition temperatures, critical micellization temperatures, and individual morphological change temperatures were found to increase on increasing the copolymer concentration. The water concentration in the DMF/water system was also crucial in these changes as it affected the mobility of the PS chains. No morphological changes can be observed when the system contained a water concentration that was higher than or equal to 10 wt %. The main driving force for these changes was analyzed to be the reduction of the free energy of the corona. When the system was isothermally kept at 50 °C after the system was rapidly heated from room temperature or cooled from high temperatures, large compound micelles were observed as an intermediate or metastable morphology during the initial stage of the morphological change. Furthermore, the appearance of these intermediate or metastable micelles was isothermal condition dependent.

(50) Keller, A.; Cheng, S. Z. D. *Polymer* **1998**, *39*, 4461−4487.
(51) Cheng, S. Z. D.; Keller, A. *Ann. Rev. Mater. Sci.* **1998**, *28*, 533−562.

Acknowledgment. This work was supported by NSF (DMR-0516602).

Supporting Information Available: Experimental section, change in PS−solvent interaction parameter ($\chi_{PS-solvent}$) with temperature for different water content, TEM images for hysteresis experiments, TEM images for isothermal experiments when the sample was cooled from 65 to 50 °C, and TEM images for isothermal experiments when the sample was heated from room temperature to 70 °C. This material is available free of charge via the Internet at http://pubs.acs.org.

JA0653019